

# Low Precision Decentralized Distributed Training with Heterogeneous Data

Sai Aparna Aketi  
Purdue University  
West Lafayette, Indiana, USA - 47906.  
saketi@purdue.edu

Sangamesh Kodge  
Purdue University  
West Lafayette, Indiana, USA - 47906.  
skodge@purdue.edu

Kaushik Roy  
Purdue University  
West Lafayette, Indiana, USA - 47906.  
kaushik@purdue.edu

## Abstract

*Decentralized distributed learning is the key to enabling large-scale machine learning (training) on the edge devices utilizing private user-generated local data, without relying on the cloud. However, practical realization of such on-device training is limited by the communication bottleneck, computation complexity of training deep models and significant data distribution skew across devices. Many feedback-based compression techniques have been proposed in the literature to reduce the communication cost and a few works propose algorithmic changes to aid the performance in the presence of skewed data distribution by improving convergence rate. To the best of our knowledge, there is no work in the literature that applies and shows compute efficient training techniques such quantization, pruning etc., for peer-to-peer decentralized learning setups. In this paper, we analyze and show the convergence of low precision decentralized training that aims to reduce computational complexity of training and inference. Further, We study the effect of degree of skew and communication compression on the low precision decentralized training over various computer vision and Natural Language Processing (NLP) tasks. Our experiments indicate that 8-bit decentralized training has minimal accuracy loss compared to its full precision counterpart even with heterogeneous data. However, when low precision training is accompanied by communication compression through sparsification we observe 1 – 2% drop in accuracy. The proposed low precision decentralized training decreases computational complexity, memory usage, and communication cost by  $\sim 4\times$  while trading off less than a 1% accuracy for both IID and non-IID data. In particular, with higher skew values, we observe an increase in accuracy (by  $\sim 0.5\%$ ) with low precision training, indi-*

*cating the regularization effect of the quantization.*<sup>1</sup>

## 1. Introduction

Deep learning models have achieved exceptional performance in many computer vision, natural language processing (NLP) and reinforcement learning (RL) tasks. This remarkable success is largely attributed to the availability of humongous amounts of data and computational power. These models are traditionally trained on a single system or a cluster of nodes by centralizing data from various distributed sources or edge devices. This results in transferring tremendous amount of information to data-centers or the cloud and subsequently train the models using enormous computational power. Such centralized computing, even though successful in some industrial use cases, requires large amount power and network bandwidth for transfer of data from edge devices and also increases users' privacy concerns. This fundamentally limits the amount of data that can be collected and used for training the more intelligent and generalized models. In order to handle this problem, a new interest in developing distributed learning algorithms has emerged. A well-known distributed optimization setting in machine learning is federated learning or centralized distributed learning [10]. The idea here is to keep the training data locally at the edge devices and learn shared global model by aggregating the locally computed updates through a central coordinating server. This avoids the logging of user data to a data center and helps safeguard users' privacy. However, communication traffic jam at the central server and a single point of failure becomes a potential bottleneck for such centralized settings. This has motivated

<sup>1</sup>Our code is available at [https://github.com/aparna-aketi/Low\\_Precision\\_DL](https://github.com/aparna-aketi/Low_Precision_DL)

the advancements in decentralized distributed learning algorithms where each node communicates only with its neighbours eliminating the requirement of a central server.

*Key Challenges in On-Device Decentralized Learning:* There are three main challenges in realizing decentralized training on edge devices. Training a model over decentralized peer-to-peer learning using traditional algorithms such as D-PSGD [12] requires massive amounts of communication. Second, deep learning models are usually very compute heavy and training such models on resource constrained edge devices is infeasible. Lastly, the training data on each device is based on the behaviour and preference of the user and this can lead to significant differences in the data distribution across the devices depending on the user pool. However, most of the existing works [8, 9, 15, 17, 19] only focus on communication compression assuming the data partitions to be independent and identically distributed (IID). Even though [6, 13] deal with heterogeneous (or non-IID) data, they either do not analyse it in the presence of communication compression or peer-to-peer decentralized setup where each node only communicates with its neighbours. This leaves us with an important question: *What is the effect of heterogeneous data partitions on compute and communication efficient peer-to-peer decentralized machine learning?*

In this paper, we aim to show the convergence of compute efficient low precision (8-bit) training and analyze the effect of communication compression over state-of-the-art decentralized algorithms with heterogeneous data distribution. We mainly focus on a common type of heterogeneous data, widely used in prior work [6, 20, 22]: skewed distribution of data labels across devices. We evaluate two popular decentralized algorithms, Deep-Squeeze [19] and CHOCO-SGD [8], on various applications and architectures. Since the above mentioned algorithms converge only for undirected graphs, we modify them to include Push-Sum technique [2] similar to [1, 18] removing the constraint of requiring symmetric and doubly stochastic graph topologies. For our analysis, we extend the single node low precision 8-bit training technique proposed in [3] for decentralized training setups. Since 'Batch-Norm' layer is not well suited for low precision training [3] and for decentralized learning with heterogeneous data [6], we propose 'Range EvoNorm' by combining the concepts of 'Range Batch-Norm' [3] and S0 variant of 'EvoNorm' [14]. We empirically show that low precision training converges in the decentralized case and has minimal drop in accuracy as compared to its full precision training counterpart. The degree of skew in the data partitions has very similar effect on low-precision and full-precision training. We further observe that low precision training with optimal models (e.g., ResNet-20 for CIFAR-10) improves accuracy slightly ( $\sim 1\%$ ) compared to full precision training under high degree of skew. We claim

that the improvement is potentially due to the regularization effect of the low precision training. We further replace the local momentum with Quasi-Global (QG) momentum as suggested in [13] to improve the accuracy by  $1 - 2\%$  for decentralized setups with heterogeneous data.

### 1.1. Contributions:

We make the following contributions.

- We show the convergence of low precision (8-bit) training with decentralized learning setup through a detailed study. Our experiments evaluate the feasibility of low precision decentralized training on various image classification and natural language processing tasks. To the best of our knowledge, this is the first time that low precision training has been applied to decentralized learning setup.
- We propose 'Range EvoNorm' which is better suited for low precision decentralized implementation over both IID and non-IID data partitions. It replaces the variance (of activations computer per instance) term in the S0 variant of EvoNorm [14] with a scaled range of the activations, and sigmoid non-linearity by hard-sigmoid activation.
- We analyze the effect of data skew and communication compression on low precision decentralized training. We observe that the low precision training with optimal networks improves the accuracy by  $0.5\% - 1\%$  under high degree of data skew and no communication compression. We speculate that the regularization effect of the low precision training is counter-acting the over-fitting of the model to the local data causing the accuracy improvements.

## 2. Background

In this section, we provide the background on decentralized peer-to-peer learning algorithms.

*Decentralized Learning:* In decentralized learning, the aim is to train a machine learning model with parameter vector  $x$  using all the training samples that are generated and stored across  $n$  edge devices. The end goal is to learn one model that fits all the training samples without sharing the local data. This is usually achieved by combining a local stochastic gradient descent with global consensus based optimization such as gossip averaging [12]. The nodes/devices are connected via a weighted, sparse, yet strongly connected graph topology. Traditionally, most decentralized learning algorithms assume the data samples to be independent and identically distributed (IID) among different devices, and this is referred as the IID setting. Conversely, we refer Non-IID/heterogeneous settings as the one for which the above assumption does not hold.

In this paper, we show the convergence of decentralized low precision training by evaluating it using two popular algorithms on different applications over IID and Non-IID settings. Both the algorithms use gossip based global averaging with stochastic gradient descent and aim to reduce communication by sending compressed model weights or gradients to the neighbours. The following are the details of these algorithms.

- *Deep-Squeeze* [19] employs error compensated communication compression to a gossip based decentralized learning setup. Without communication compression, Deep-Squeeze is the same as Decentralized Parallel Stochastic Gradient Descent (D-PSGD) proposed in [12]. Any given device (say  $i$ ) updates its model weights  $x_i$  locally using SGD and then communicates only the top- $k\%$  of the error compensated weights to the neighbours. Every local update step is followed by a gossip averaging step where each node updates the model with a weighted average of all the communicated models (from its neighbours) including itself. (Algorithm 2 in the Supplementary material)
- *CHOCO-SGD* [8]: is another gossip-based stochastic gradient descent algorithm that communicates compressed model updates (i.e.  $x_i^t - x_i^{t-1}$ ) rather than the model weights. They achieve this by introducing an additional buffer  $\hat{x}_i$  that acts as a proxy to the model weights  $x_i$ . The  $\hat{x}_i$ 's are available to all the neighbours of the node  $i$  and referred as the 'publicly available' copies of private  $x_i$ . The compressed gradients received from a neighbor  $j$  to  $i$  are used to update  $\hat{x}_j$  at node  $i$  and the gossip averaging step averages  $x_i$  and  $\hat{x}_j$ 's. In general  $x_i \neq \hat{x}_i$ , due to the communication restriction. Since CHOCO-SGD communicates only gradients (in particular, model updates) and the gradients converge to zero as the training converges, we expect it to perform better than Deep-squeeze. (Algorithm 3 in the Supplementary material)

Both the above mentioned algorithms assume the data partitions to be IID and the mixing matrix (adjacency matrix  $W$ ) of the decentralized setup to be symmetric and doubly stochastic. Doubly stochastic constraint requires every row and column to sum to 1. The authors in [1] propose Sparse-Push combining deep-squeeze algorithm with Stochastic Gradient Push (SGP) [2] which allows the training to converge for directed and time varying graphs reducing the constraint on mixing matrix to be only column stochastic. Quant-SGP [18] extended D-PSGD to directed graphs by effectively combining SGP algorithm with CHOCO-SGD. In this paper, we will show the convergence of low precision decentralized training over directed graphs with heterogeneous data using Quant-SGP variant of CHOCO-SGD and Sparse-Push variant of Deep-Squeeze.

### 3. Decentralized Low Precision Training

In this section, we describe our low precision training methodology for decentralized learning setup over IID and non-IID data partitions.

*Decentralized Setup:* We consider a decentralized peer-to-peer learning problem with  $n$  nodes connected over a directed and weighted graph topology  $G = (n, E)$  where  $E$  are the set of edges. The edge  $(i, j) \in E$  indicates that node  $i$  communicates information to node  $j$ . We represent  $N(i)$  as the in-neighbours of  $i$  including itself i.e. set of nodes with incoming edge to  $i$ . Additionally, we assume that the graph  $G$  is strongly-connected (there is a path from every node to every other node) and has self-loops. The adjacency matrix of the graph  $G$  is referred as a mixing matrix  $W$  where  $W_{ij}$  is the weight associated with edge  $(i, j)$ . The values of weights lie in the interval of  $[0, 1]$ . Note that a weight 0 indicates the absence of an edge and a non-zero weight indicate the weightage given to model at node  $j$  while being averaged at node  $i$ . The weight matrix is assumed to be column stochastic i.e. the columns sum to 1. Further, each node has its own local data coming from distribution  $D_i$  and an initial model estimate  $x_i^{(0)}$ . Our aim is to solve the optimization problem of minimizing global loss function  $f(x)$  distributed across  $n$  nodes as given in equation. 1. Note that  $F_i$  is a local loss function at node  $i$  (for example, cross entropy loss).

$$\min_{x \in \mathbb{R}^d} f(x) = \frac{1}{n} \sum_{i=1}^n f_i(x), \quad (1)$$

and  $f_i(x) = \mathbb{E}_{\xi_i \in D_i} [F_i(x_i, \xi_i)] \quad \forall i$

*Decentralized Training:* Communication efficient decentralized training algorithms such as CHOCO-SGD and Deep-Squeeze usually have four stages in each iteration of the training as shown in Algorithm. 1. (1) *Local computation stage:* Compute the stochastic gradient descent updates for each node using a randomly selected batch from the local data. (2) *Compression stage:* Compress the model weights/model-updates based on a given compression operator. In case of Deep-Squeeze, error compensated weights (models weights with accumulated compression error) are compressed. In contrast, CHOCO-SGD compresses the change in model weights from the previous communication step. (3) *Communication stage:* The compressed information from each node  $i$  is sent to its neighbors, namely  $N(i)$ . (4) *Gossip update stage:* Each node updates its local model by performing a gossip update utilizing the information received from its neighbors – a neighbourhood weighted averaging. The predefined function  $g, h$  introduced in Algorithm. 1 are described in detail for Deep-Squeeze and CHOCO-SGD in supplementary material.

*Low Precision Training:* We extend the single node 8-bit training proposed in [3] to peer-to-peer decentralized learn-

---

**Algorithm 1** Decentralized Peer-to-Peer Training

---

**Input:** Each node  $i$  initializes model weights  $x_i^{(0)}$ , learning rate  $\gamma$ , averaging rate  $\eta$ , mixing matrix  $W$ , and compression operator  $C$ , predefined functions  $g, h$ .

1. **for**  $t=0, 1, \dots, T-1$  **do**

Each node simultaneously implements:

2. Compute the local gradients:  $g_i^{(t)} = \nabla F_i(x_i^{(t)}, \xi_i^{(t)})$
  3. Update the model:  $\tilde{x}_i^{(t)} = x_i^{(t)} - \eta g_i^{(t)}$
  4. Compute  $v_i^{(t)} = g(\tilde{x}_i^{(t)})$  that has to be communicated.
  5. Compress the information  $C[v_i^{(t)}]$
  6. Communicate  $C[v_i^{(t)}]$  to neighbors  $N(i)$ .
  7. Update the model by weighted gossip averaging step:  
 $x_i^{(t+1)} = \tilde{x}_i^{(t)} + \gamma \sum_{j \in N(i)} W_{ij} * h(C[v_j^{(t)}])$
  8. **end**
- 

ing setups. This training methodology uses GEMMLOWP integer quantization scheme as described in Google’s open source library [4]. In every iteration of training, we quantize the weights, activations, as well as a substantial volume of the gradients stream, in all layers including normalization layer to 8-bit across all nodes. The back-propagation phase requires twice the number of multiplications compared to the forward pass and hence, quantization of gradients is crucial for accelerating the training. Quantizing the entire backward phase results in significant degradation of accuracy and it has been empirically shown in [3] that gradient bifurcation during 8-bit training is critical for high accuracy results. Each layer derives two sets of gradients for the weight update i.e., the layer gradients ( $g_l$ ) for the backward propagation that are passed to the previous layer and the weight gradients ( $g_{W_l}$ ) that are used to update the weights in the current layer. In gradient bifurcation, only the layer gradients  $g_l$  are quantized to 8-bits integers while the weight gradients  $g_{W_l}$  are either 16-bit or 32-bit float. In our implementation, gradient bifurcation takes place during the backward pass at each node. Similar to 8-bit single node training in [3], we used the most simple and hardware friendly approach of straight-through estimator (STE) to approximate differentiation through discrete variables.

$$\text{Sigmoid}(x) = \frac{1}{1 + e^{-x}} \tag{2}$$

$$\text{Hard-Sigmoid}(x) = \max\left(0, \min\left(1, \frac{x+3}{6}\right)\right)$$

Other computations, apart from gradients that can cause numerical instability, are the batch-normalization layers. A traditional implementation of batch-norm includes the computation of the sum of squares, square-root and reciprocal operations which require high precision and high dynamic range. A replacement for batch-norm layer is range batch-norm, that normalizes inputs by the range of the input dis-

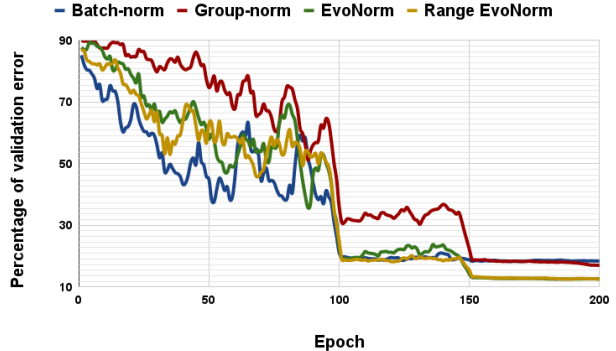


Figure 1. Plot showing the validation error during training of CIFAR-10 dataset on ResNet-20 architecture with various normalization layers over 8 node directed ring topology and a degree of skew of 0.8.

tribution (i.e.,  $\max(x) - \min(x)$ ) across the batch. This has been shown to be more suitable for low precision implementations in [3]. However, in decentralized learning setup with heterogeneous data, batch-norm often fails due to the discrepancies between local activation statistics across the nodes [6]. As a counteractive measure, the authors in [13] propose to replace batch-norm with S0 variant of EvoNorm [14] as it does not use the run-time batch statistics. Figure. 1 verifies that EvoNorm indeed performs better than batch-norm or group-norm in the presence of heterogeneous data. Combining the concepts of range batch-norm and EvoNorm, we propose ‘Range Evonorm’ that normalizes inputs by the range of activation distribution of each input. We also replace the sigmoid function with hard-sigmoid shown in equation. 2 to avoid the computation of exponential function which requires high precision. This ensures that the normalization layer uses sample statistics rather than batch statistics during training. It also avoids computing sum of squares and square-roots which need high precision operations. Figure. 1 shows the equivalence of ‘Evonorm’ and ‘Range EvoNorm’ when models are trained on high precision on a decentralized setup.

## 4. Experimental Setup and Results

We study three different dimensions: 1) communication efficient decentralized learning algorithms 2) degree of skew and 3) various ML applications and models. We explore all the dimensions with rigorous experimental methodologies. In particular, we focus on showing the convergence of low precision decentralized training and the effect of the above three dimensions on the performance of such training. We experiment on two dominant ML applications – image recognition and NLP, various DNN structures, and datasets. For all the experiments we replace batch-norm

+ ReLU layers with  $S0$  variant on EvoNorm for full precision training and Range EvoNorm for low precision 8-bit training. The baseline accuracies for all the datasets and architectures trained on a single node with entire dataset are reported in Table. 1. In all the tables: DS, LP-DS indicates Deep-Squeeze (full precision) [19] and our Low Precision Deep-Squeeze respectively; CHOCO and LP-CHOCO represents CHOCO-SGD (full precision) [8] and our Low Precision CHOCO-SGD, respectively; QGM is Quasi-Global Momentum [13]. The performance is measured in terms of the test accuracy of the averaged model across all nodes.

Table 1. Baseline accuracy of training on a single node. Acc. (FP) indicates test accuracy (%) with full precision training and Acc. (LP) indicates test accuracy with low precision (8-bit) training.

Dataset	Model	Params (M)	Acc. (FP)	Acc. (LP)
CIFAR10	ResNet-20	0.27	91.25	91.12
CIFAR10	ResNet-54	0.76	91.99	91.66
CIFAR10	VGG-11	9.49	89.59	89.78
Imagenette	ResNet-18	11.2	87.26	87.26
Imagenette	VGG-11	9.49	89.58	87.39
AGNews	DistillBERT	66.7	94.47	93.89
Sentlen	DistillBERT	66.7	99.17	99.36

#### 4.1. Computer Vision Tasks

We evaluate the performance of low precision decentralized training on image recognition task using CIFAR-10 [11] and a subset of ImageNet [7] datasets with ResNet and VGG architectures over ring and Torus graph topologies. We modify the linear layers of VGG-11 to contain a hidden size of 512 and output size of 10.

*CIFAR-10 Dataset:* CIFAR-10 is a 10-class image classification dataset with 50,000 train samples and 10,000 test samples each with a resolution of  $32 \times 32$ . The train and test samples are distributed nearly equally across the 10 classes. The experiments were conducted on multiple graph structures such as directed ring topology (one peer per node) with 8, 16 nodes and undirected Torus (four peers per node) topology with 16 nodes. Note that the spectral gap of 16 node directed ring is same as 32 node undirected ring. We use ResNet-20, ResNet-54 and VGG-11 for evaluating CIFAR-10 dataset and the results are shown in Table. 2. All the experiments were run for 200 epochs. We use an initial learning rate of 0.1 decayed by a factor of 10 at epoch 100, 150 for ResNet architectures and decayed by factor of 2 every 30 epochs for VGG-11. We have used layer-wise top-K sparsification compressor for communication compression – for example, 99% compression indicates that top 1% of the weight from each layer are communicated. We experiment with four different degree of skews (0, 0.4, 0.8, 0.9)

and the distribution of classes across the nodes for these skews is shown in Fig. 2. Note that skew of 0 represents IID data partitions across the nodes.

*Imagenette Dataset:* Imagenette is a subset of Imagenet and is a 10-class image classification dataset with 9,469 training samples and 3,925 test samples each, with a resolution of  $224 \times 224$ . The train and test samples are distributed nearly equally across the 10 classes. The experiments were conducted on directed ring topology (one peer per node) with 4 nodes and on undirected Torus (four peers per node) topology with 8 nodes. We use ResNet-18 and VGG-11 architectures for evaluating this dataset and the results are shown in Table. 4. Note that we only show the performance of CHOCO-SGD in Table. 4 as it performs better than Deep-Squeeze. All the experiments were run for 100 epochs. An initial learning rate of 0.1 decayed by a factor of 10 at epoch 50, 75 was used for ResNet-18 and an initial learning rate of 0.01 decay by factor of 2 every 30 epochs for VGG-11. We experiment with two different degrees of skew – 0 (IID), 0.6 (non-IID). We have used layer-wise top-K sparsification compressor for communication compression.

Our experiments show that low precision decentralized training converges for both IID and Non-IID data partitions as long as the full precision training converges for similar data partitions. The low precision training with full communication (0% compression) has minimal accuracy loss of less than 1% compared to full precision training. In the presence of communication compression, low precision training has 1 – 2% loss in accuracy depending on the graph size, connectivity and percentage of compression. We also observe that for higher degree of skew (0.9), low precision training performs better than full precision training. For CIFAR-10 dataset trained on ResNet-20, LP-CHOCO shows an improvement of 0.56%, 0.83% over 8-node and 16-node directed ring topology, respectively. The potential reason for this behaviour is the regularization effect of the low precision training. With higher skew values, the local models can easily overfit the local data and hence, regularizing the weights while training can result in better performance. We also test the low precision decentralized training with QG momentum [13] shown in Table. 3. We observe that low precision training has similar improvements with skew as compared to full precision and hence, QG momentum can be used in synergy with our proposed training methodology.

We show the scalability of the proposed low precision decentralized training by evaluating more complex dataset such as Imagenette. Even though Imagenette has 10 classes, it is a complex dataset compared to CIFAR-10 because of the higher resolution and lower training set size. Since Imagenette has less samples per class in the training set (around 1000 per class), we used lower degree of skew (0.6) com-

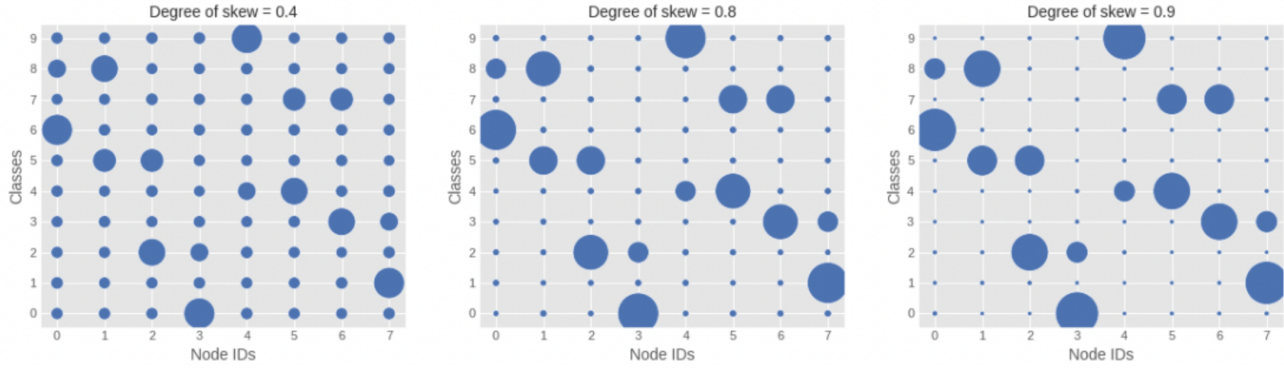


Figure 2. The distributions of CIFAR-10 classes across 8 nodes in a ring topology with various degree of skew in the partition.

Table 2. Decentralized training of CIFAR-10 dataset over various graph topologies and model architectures.

Model/ Graph	Nodes (n)	Compression (%)	Degree of skew	DS (32-bit)	LP-DS (8-bit)	CHOCO (32-bit)	LP-CHOCO (8-bit)
ResNet-20/ Directed Ring	8	0	0	90.56	90.57	<b>90.96</b>	90.30
			0.4	90.36	89.89	<b>90.37</b>	90.29
			0.8	87.57	87.68	<b>87.87</b>	87.06
			0.9	83.82	82.94	83.09	<b>83.65</b>
	99	0	88.67	87.58	<b>89.21</b>	88.23	
		0.4	<b>88.64</b>	88.02	88.58	88.44	
		0.8	85.43	84.44	<b>85.78</b>	84.79	
		0.9	82.94	81.92	<b>83.49</b>	82.22	
	16	0	0	89.92	89.30	90.23	<b>90.26</b>
			0.4	88.88	87.85	<b>90.01</b>	89.59
			0.8	85.21	85.39	<b>86.47</b>	86.47
			0.9	77.16	77.57	78.70	<b>79.53</b>
90	0	86.58	85.45	<b>88.43</b>	87.72		
	0.4	85.92	84.67	<b>87.98</b>	86.85		
	0.8	80.60	79.44	<b>82.76</b>	80.24		
	0.9	76.44	73.69	<b>77.42</b>	74.66		
ResNet-54/ Directed Ring	8	0	0	91.33	<b>92.09</b>	91.80	91.44
			0.4	91.40	91.28	<b>91.45</b>	91.19
			0.8	89.72	88.98	<b>90.19</b>	89.30
			0.9	87.15	84.06	87.17	<b>87.40</b>
	99	0	<b>90.23</b>	88.57	89.44	88.85	
		0.4	89.48	88.60	<b>89.31</b>	88.81	
		0.8	85.91	84.69	<b>86.57</b>	85.06	
		0.9	<b>83.61</b>	81.93	83.27	81.87	
VGG-11/ Undirected Torus	16 (4x4)	0	0	89.64	89.13	<b>90.21</b>	89.73
			0.4	89.47	89.21	89.49	<b>89.80</b>
			0.8	87.20	86.67	<b>87.21</b>	86.73
			0.9	86.26	85.15	<b>86.66</b>	85.67
	99	0	86.10	82.70	<b>86.72</b>	84.44	
		0.4	85.42	81.53	<b>86.01</b>	83.49	
		0.8	80.12	77.98	<b>81.25</b>	80.53	
		0.9	77.10	72.89	<b>77.94</b>	76.11	

Table 3. Results of training CIFAR-10 dataset on ResNet-20 architecture over 8-node directed topology using Quasi-Global Momentum and CHOCO-SGD (both low and full precision).

Compression (%)	Degree of skew	CHOCO with QGM	LP-CHOCO with QGM
0	0.0	91.07	90.20
	0.4	90.64	90.10
	0.8	87.64	87.16
	0.9	84.49	<b>85.28</b>
99	0.0	89.87	89.12
	0.4	89.39	88.73
	0.8	86.76	85.52
	0.9	84.42	83.68

Table 4. Decentralized training on Imagenette dataset (Subset of Imagenet with 10 classes) over different graph topologies.

Model/ Graph (n)	Comp. (%)	Skew	CHOCO (32-bit)	LP-CHOCO (8-bit)
ResNet-18/ Torus (8)	0	0.0	87.10	86.60
		0.6	85.58	84.20
	90	0.0	85.25	83.17
VGG-11/ Ring (4)	0	0.0	89.76	88.49
		0.6	88.89	86.82
	90	0.0	88.92	87.25
		0.6	88.20	86.27

pared to CIFAR-10 to evaluate the Non-IID case. Note that a skew of 0.6 for imagenette has same impact as skew of 0.8 for CIFAR-10 in terms of data distribution. Table. 4 shows that the low precision training converges even for complex datasets and large models over both IID and Non-IID data partitions. Therefore, the proposed low precision decentralized training trades-off of 1 – 2% accuracy for  $\sim 4\times$  reduction in computation and memory cost during training and inference along with  $4\times$  faster inference.

## 4.2. Natural Language Processing Tasks

We analyze the effect of low precision training on natural language processing task for AG News [21] and Sentlen from the probing dataset in SENEVAL framework [5] with DistillBERT [16] as our base model. Our experimental setup consists of 4 nodes connected through directed ring topology. We evaluate low precision training with Deep-Squeeze and CHOCO-SGD for three different degrees of skews (0.0, 0.5, 0.9) and two different compression ratios (0%, 99%). Both the datasets are fine tuned for 5 epochs with Adam optimizer and a learning rate,  $\beta_1$ ,  $\beta_2$  and weight decay of  $3 \times 10^{-5}$ , 0.9, 0.9, and  $1 \times 10^{-4}$  respectively.

*AG News Dataset:* AG News dataset [21] is a 4

way classification dataset constructed by assembling titles and description fields of the articles from the 4 largest classes ('Sports', 'Sci/Tech', 'Business', 'World') of AG's News Corpus <sup>2</sup>. The dataset consists of 120000 training samples and 7600 test samples distributed equally across the 4 classes.

*Sentlen task:* Sentlen task from the probing dataset in the SentEVAL framework [5] is a 6 way classification task with the goal to predict the length of the sentences. The 6 classification bins are formed by sentence lengths belonging to the intervals 5-8, 9-12, 13-16, 17-20 21-25 and 26-28. The task consists of 100,000 training and 10,000 validation samples distributed nearly equally across the 6 classes.

The results for the NLP experiments are presented in Table. 5. Low precision training has less than 1% drop in accuracy as compared to full precision counterpart for both Deep-Squeeze and ChOCO-SGD. We do not observe the regularization effect of low precision training for higher degree of skew (0.9) seen in Vision tasks. This can be potentially due to the large size of the model masking the effects of regularization through low precision training.

## 5. Hardware Implications

Let us discuss the energy and memory benefits of low precision training. During the training of a deep learning model, majority of the memory usage comes from storing the activations of the batch of images to compute the gradients. Data-parallel distributed learning reduces this memory requirement by lowering the batch-size per device, which in turn decreases the computations per iteration while still keeping the throughput constant. However, this has no effect on network size and each node has to still store and access the millions of parameters of a deep neural network. The network size can be reduced by employing low precision decentralized training which quantizes the weights and activations to 8-bits. This further reduces the total compute and memory requirement enabling training on resource constrained edge devices such as drones, smartphones etc. Figure. 3 illustrates the memory and compute required to train a full/high precision and a low precision ResNet-20 model on CIFAR-10 dataset over a decentralized setup. Low precision training can reduce the compute and communication cost by  $\sim 4\times$  and memory requirements by  $3.5\times$ . In particular, we use integer quantization which results in integer operations that are more efficient than float operations. Notably, low precision inference also reduces the compute, memory and latency  $4\times$  due to the quantization of weights to 8 bits.

<sup>2</sup>[http://groups.di.unipi.it/~gulli/AG\\_corpus\\_of\\_news\\_articles.html](http://groups.di.unipi.it/~gulli/AG_corpus_of_news_articles.html)

Table 5. Decentralized training of various Natural Language Processing (NLP) tasks over a directed 8 node ring topology.

Dataset/ Model	Compression (%)	Degree of skew	DS (32-bit)	LP-DS (8-bit)	CHOCO (32-bit)	LP-CHOCO (8-bit)
AGNews/ DistillBERT	0	0.0	94.18	93.99	<b>94.21</b>	94.12
		0.5	94.13	93.72	<b>94.15</b>	93.61
		0.9	<b>92.19</b>	91.35	91.56	91.49
	99	0.0	93.88	93.55	<b>94.54</b>	94.04
		0.5	93.41	92.92	<b>93.83</b>	93.22
		0.9	91.93	91.21	<b>92.33</b>	91.80
Sentlen/ DistillBERT	0	0.0	99.39	98.83	<b>99.48</b>	98.75
		0.5	99.54	98.92	<b>99.55</b>	99.00
		0.9	<b>99.39</b>	98.46	99.33	98.32
	99	0.0	98.67	98.24	<b>99.10</b>	98.59
		0.5	98.66	97.94	<b>98.95</b>	98.55
		0.9	98.04	97.28	<b>98.72</b>	97.73

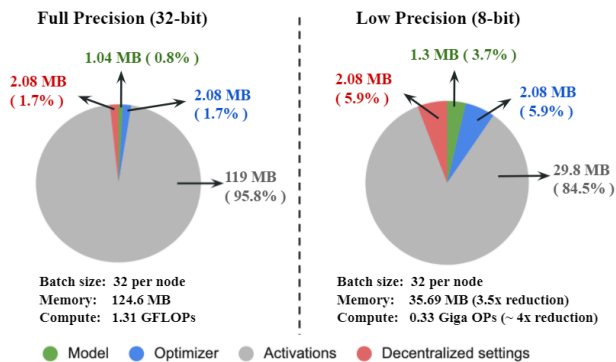


Figure 3. Memory and compute requirements for each node per iteration of full precision vs low precision training of CIFAR-10 dataset on ResNet-20 architecture over a decentralized setup.

## 6. Limitations

From the series of experiments with various datasets, architectures and graph topologies, we found the following limitations with communication and compute efficient decentralized learning. The performance (accuracy) decreases with increase in the degree of skew in the data partitions across the nodes. When low precision training is accompanied by communication compression, it incurs  $\sim 1 - 2\%$  more degradation in accuracy (in most cases) compared to full communication. Apart for data and model complexity, various decentralized graph parameters such as graph size, spectral gap (connectivity of the graph) and percentage of communication compression also play a role in determining the tolerable amount of skew for a given decentralized learning task. This makes it harder to predict the trends in performance with varying degree of skew. In most of the cases, the models do not converge (for both full precision and low precision training) for a skew of 1 (100% non-IID)

i.e., every node has data belonging to unique classes. Our study shows that CHOCO-SGD performs better than Deep-Squeeze. However, CHOCO-SGD needs additional memory buffer on each node with size equivalent to model size.

## 7. Conclusion

Efficient decentralized distributed learning with practical constraints is the key to training intelligent deep learning models on edge devices. In this paper, we conduct a detailed study to reveal and understand the effect of various factors on low precision decentralized learning. We analyze the convergence of low precision training under the variation of several key factors such as the learning algorithm (CHOCO-SGD and Deep-Squeeze), degree of skew, communication compression. We evaluated the effect of all the above factors over a considerable number of tasks, datasets, models and graph topologies. The following are the key findings from our study: 1) Our experiments show that low precision decentralized learning converges with minimal loss in accuracy compared to full precision training. This reduces the compute during training and inference by  $\sim 4\times$  while making inference  $4\times$  faster. 2) A suitable normalization layer that works better with both quantization and heterogeneous data is ‘Range Evonorm’. 3) Decentralized algorithms that communicate the gradients (such as CHOCO-SGD) at the cost of additional memory buffer, perform better in terms of accuracy than algorithms that communicate the weights such as Deep-Squeeze. 4) We observe that there is a slight improvement in accuracy for low precision training compared to full precision in the presence of high skew (0.9) and no communication compression. This is due to the regularization effect of the low precision training. 5) We also show the effect of communication compression with increasing skew for both full precision and low precision training. We hope that the findings and insights in this paper will help in



better understanding of efficient decentralized learning over heterogeneous data and spur further research in the fundamental problem of heterogeneous (non-IID) data in decentralized learning.

## References

- [1] Sai Aparna Aketi, Amandeep Singh, and Jan Rabaey. Sparse-push: Communication- & energy-efficient decentralized distributed learning over directed & time-varying graphs with non-iid datasets, 2021. [2](#), [3](#), [11](#)
- [2] Mahmoud Assran, Nicolas Loizou, Nicolas Ballas, and Mike Rabbat. Stochastic gradient push for distributed deep learning. In *Proceedings of the 36th International Conference on Machine Learning*, volume 97 of *Proceedings of Machine Learning Research*, pages 344–353. PMLR, 09–15 Jun 2019. [2](#), [3](#)
- [3] Ron Banner, Itay Hubara, Elad Hoffer, and Daniel Soudry. Scalable methods for 8-bit training of neural networks. In *Advances in Neural Information Processing Systems*, volume 31. Curran Associates, Inc., 2018. [2](#), [3](#), [4](#)
- [4] J Benoit, W Pete, and W Miao. gemmlowp: a small self-contained low-precision gemm library. <https://github.com/google/gemmlowp>, 2017. [4](#)
- [5] Alexis Conneau and Douwe Kiela. Senteval: An evaluation toolkit for universal sentence representations. *arXiv preprint arXiv:1803.05449*, 2018. [7](#)
- [6] Kevin Hsieh, Amar Phanishayee, Onur Mutlu, and Phillip Gibbons. The non-IID data quagmire of decentralized machine learning. In *Proceedings of the 37th International Conference on Machine Learning*, volume 119 of *Proceedings of Machine Learning Research*, pages 4387–4398. PMLR, 13–18 Jul 2020. [2](#), [4](#)
- [7] Hamel Husain. Imagenette - subset of 10 easily classified classes from imagenet. <https://github.com/fastai/imagenette>, 2018. [5](#)
- [8] Anastasia Koloskova, Tao Lin, Sebastian U Stich, and Martin Jaggi. Decentralized deep learning with arbitrary communication compression. *International Conference on Learning Representations*, 2020. [2](#), [3](#), [5](#), [10](#)
- [9] Anastasia Koloskova, Sebastian Stich, and Martin Jaggi. Decentralized stochastic optimization and gossip algorithms with compressed communication. In *Proceedings of the 36th International Conference on Machine Learning*, volume 97 of *Proceedings of Machine Learning Research*, pages 3478–3487. PMLR, Jun 2019. [2](#)
- [10] Jakub Konečný, H Brendan McMahan, Daniel Ramage, and Peter Richtárik. Federated optimization: Distributed machine learning for on-device intelligence. *arXiv preprint arXiv:1610.02527*, 2016. [1](#)
- [11] Alex Krizhevsky, Vinod Nair, and Geoffrey Hinton. Cifar-10 (canadian institute for advanced research). <http://www.cs.toronto.edu/~kriz/cifar.html>, 2014. [5](#)
- [12] Xiangru Lian, Ce Zhang, Huan Zhang, Cho-Jui Hsieh, Wei Zhang, and Ji Liu. Can decentralized algorithms outperform centralized algorithms? a case study for decentralized parallel stochastic gradient descent. In *Advances in Neural Information Processing Systems*, volume 30, 2017. [2](#), [3](#)
- [13] Tao Lin, Sai Praneeth Karimireddy, Sebastian Stich, and Martin Jaggi. Quasi-global momentum: Accelerating decentralized deep learning on heterogeneous data. In *Proceedings of the 38th International Conference on Machine Learning*, volume 139 of *Proceedings of Machine Learning Research*, pages 6654–6665. PMLR, 18–24 Jul 2021. [2](#), [4](#), [5](#)
- [14] Hanxiao Liu, Andy Brock, Karen Simonyan, and Quoc Le. Evolving normalization-activation layers. In H. Larochelle, M. Ranzato, R. Hadsell, M. F. Balcan, and H. Lin, editors, *Advances in Neural Information Processing Systems*, volume 33, pages 13539–13550. Curran Associates, Inc., 2020. [2](#), [4](#)
- [15] Yucheng Lu and Christopher De Sa. Moniqua: Modulo quantized communication in decentralized SGD. In *Proceedings of the 37th International Conference on Machine Learning*, volume 119 of *Proceedings of Machine Learning Research*, pages 6415–6425. PMLR, Jul 2020. [2](#)
- [16] Victor Sanh, Lysandre Debut, Julien Chaumond, and Thomas Wolf. Distilbert, a distilled version of bert: smaller, faster, cheaper and lighter. *arXiv preprint arXiv:1910.01108*, 2019. [7](#)
- [17] Hossein Taheri, Aryan Mokhtari, Hamed Hassani, and Ramtin Pedarsani. Quantized decentralized stochastic learning over directed graphs. In *International Conference on Machine Learning*, pages 9324–9333. PMLR, 2020. [2](#)
- [18] Hossein Taheri, Aryan Mokhtari, Hamed Hassani, and Ramtin Pedarsani. Quantized decentralized stochastic learning over directed graphs. In *Proceedings of the 37th International Conference on Machine Learning*, volume 119, pages 9324–9333, 2020. [2](#), [3](#), [11](#)
- [19] Hanlin Tang, Xiangru Lian, Shuang Qiu, Lei Yuan, Ce Zhang, Tong Zhang, and Ji Liu. DeepSqueeze: Decentralization meets error-compensated compression, 2019. [2](#), [3](#), [5](#), [10](#)
- [20] Hanlin Tang, Xiangru Lian, Ming Yan, Ce Zhang, and Ji Liu.  $d^2$ : Decentralized training over decentralized data. In *Proceedings of the 35th International Conference on Machine Learning*, volume 80 of *Proceedings of Machine Learning Research*, pages 4848–4856. PMLR, 10–15 Jul 2018. [2](#)
- [21] Xiang Zhang, Junbo Jake Zhao, and Yann LeCun. Character-level convolutional networks for text classification. In *NIPS*, 2015. [7](#)
- [22] Yue Zhao, Meng Li, Liangzhen Lai, Naveen Suda, Damon Civin, and Vikas Chandra. Federated learning with non-iid data. *CoRR, abs/1806.00582*, 2018. [2](#)

## 8. Supplementary Material

### 8.1. Algorithmic Details

Algorithm. 2 describes the Deep-Squeeze algorithm proposed in [19] and Algorithm. 3 describes CHOCO-SGD proposed in [8]. Let  $G(V, E)$  be the decentralized graph topology and  $W$  is the mixing matrix (adjacency matrix) of the graph. The graph  $G$  contains  $n$  nodes i.e.,  $|V| = n$  and the size of  $W$  is  $n \times n$ . Both the above mentioned algorithms converge only for symmetric and doubly-stochastic mixing matrices. This results in the following constraints: 1)  $W_{ij} = W_{ji}$ , 2)  $\sum_j W_{ij} = 1 \forall i$  and 3)  $\sum_i W_{ij} = 1 \forall j$  where  $W_{ij}$  is the element in the  $i^{th}$  row and  $j^{th}$  column of  $W$ . The neighbours of each node  $i$  is given by  $N(i)$ . Note that  $N(i)$  includes  $i$ .  $I_{ij}$  represents the element in the  $i^{th}$  row and  $j^{th}$  column of an identity matrix. The compressor operator  $C$  is usually chosen as random/top-k quantization or sparfication.

---

#### Algorithm 2 Deep-Squeeze [19]

---

**Input:** On each node  $i \in [n]$  - initialize model parameters  $x_0^{(i)}$ , initialize error  $\delta_0^{(i)}$  to 0s, learning rate  $\gamma$ , averaging rate  $\eta$ , mixing matrix  $W$ , and compression operator  $C$ .

1. **for**  $t = 0, \dots, T - 1$ , at each node  $i$ , **do**  
     Each node simultaneously implements:
  2. Randomly sample a mini-batch  $\xi_t^{(i)}$  from local distribution  $D_i$
  3. Compute local gradient  $g_t^{(i)} = \nabla F_i(x_t^{(i)}, \xi_t^{(i)})$
  4. Do the local update  $\tilde{x}_t^{(i)} = x_t^{(i)} - \gamma g_t^{(i)}$
  5. Compute error compensated update  $v_t^{(i)} = \tilde{x}_t^{(i)} + \delta_t^{(i)}$
  6. Compress the error compensated variable  $C[v_t^{(i)}]$
  7. Update error  $\delta_t^{(i)} = v_t^{(i)} - C[v_t^{(i)}]$
  8. **for** each neighbour  $j$  of  $i^{th}$  node ( $j \in \mathcal{N}_i$ ) **do**  
     Send  $C[v_t^{(i)}]$  and receive  $C[v_t^{(j)}]$
  9. **end for**
  10. Do the gossip update for local models:  
      $x_{t+1}^{(i)} = \tilde{x}_t^{(i)} + \eta \sum_{j \in \mathcal{N}_i} (W_{ij} - I_{ij}) C[v_t^{(j)}]$
  11. **end for**
- 

Deep-Squeeze and CHOCO-SGD use error feedback mechanism for compression forcing the compression operator to be unbiased. This allows both the algorithms to have very high compression rates such as 90%, 99%. The averaging rate  $\gamma$  is chosen based on the percentage of compression.  $\gamma$  is 1 for no compression and decreases with increase in compression. In the main paper we use pre-define functions  $g, h$  to simplify the explanation of decentralized training. For Deep-Squeeze,  $v_t^{(i)} = g(\tilde{x}_t^{(i)}) = \tilde{x}_t^{(i)} + \delta_t^{(i)}$  and  $h(C[v_t^{(j)}]) = C[v_t^{(j)}]$ . Similarly for CHOCO-SGD, we

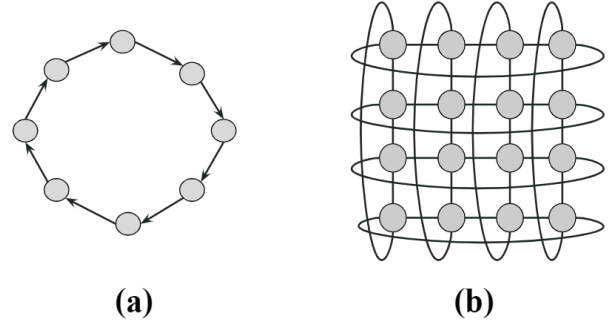


Figure 4. Graph topologies used in the decentralized experiments: (a) 8-node directed ring, and (b) 16-node (4x4) undirected Torus.

have  $v_t^{(i)} = g(\tilde{x}_t^{(i)}) = \tilde{x}_t^{(i)} - \hat{x}_t^{(i)}$ ,  $C[v_t^{(i)}] = q_t^{(i)}$  and  $h(q_t^{(j)}) = \hat{x}_{t+1}^{(j)} - \hat{x}_{t+1}^{(i)}$ .

In our experiments, we use the Sparse-Push version of Deep-Squeeze (shown in Algorithm. 4) and Quant-SGP version of CHOCO-SGD (shown in Algorithm. 5). Sparse-Push and Quant-SGP requires the mixing matrix to be column stochastic ( $\sum_i W_{ij} = 1 \forall j$ ) removing the stronger constraint of symmetry and doubly stochasticity. This enables both the algorithms to converge for directed and time-varying graphs which is more practical.

---

#### Algorithm 3 CHOCO-SGD [8]

---

**Input:** On each node  $i \in [n]$  - initialize model parameters  $x_0^{(i)}$ , initialize  $\hat{x}_0^{(j)} \forall j \in N(i)$  to 0s, learning rate  $\gamma$ , averaging rate  $\eta$ , mixing matrix  $W$ , and compression operator  $C$ .

1. **for**  $t = 0, \dots, T - 1$ , at each node  $i$ , **do**  
     Each node simultaneously implements:
  2. Randomly sample a mini-batch  $\xi_t^{(i)}$  from local distribution  $D_i$
  3. Compute local gradient  $g_t^{(i)} = \nabla F_i(x_t^{(i)}, \xi_t^{(i)})$
  4. Do the local update  $\tilde{x}_t^{(i)} = x_t^{(i)} - \gamma g_t^{(i)}$
  5. Compute and compress the sending information:  
      $q_t^{(i)} = C[\tilde{x}_t^{(i)} - \hat{x}_t^{(i)}]$
  7. **for** each neighbour  $j$  of  $i^{th}$  node ( $j \in \mathcal{N}_i$ ) **do**  
     Send  $q_t^{(i)}$  and receive  $q_t^{(j)}$   
      $\hat{x}_{t+1}^{(j)} = q_t^{(j)} + \hat{x}_t^{(j)}$
  8. **end for**
  9. Do the gossip update for local models:  
      $x_{t+1}^{(i)} = \tilde{x}_t^{(i)} + \eta \sum_{j \in \mathcal{N}_i} (W_{ij} - I_{ij})(\hat{x}_{t+1}^{(j)} - \hat{x}_{t+1}^{(i)})$
  11. **end for**
-

**Algorithm 4** Sparse-Push [1] (Deep-Squeeze with SGP)

**Input:** On each node  $i \in [n]$  - initialize model parameters  $x_0^{(i)}, z_0^{(i)} = x_0^{(i)}$ , initialize error  $\delta_0^{(i)}$  to 0s and bias weight  $u_0^{(i)}$  to 1, learning rate  $\gamma$ , averaging rate  $\eta$ , mixing matrix  $W$ , and compression operator  $C$ .

1. **for**  $t = 0, \dots, T - 1$ , at each node  $i$ , **do**  
Each node simultaneously implements:
2. Randomly sample mini-batch  $\xi_t^{(i)}$  from local distribution  $D_i$
3. Compute local gradient  $g_t^{(i)} = \nabla F_i(z_t^{(i)}, \xi_t^{(i)})$
4. Do the local update  $\tilde{x}_t^{(i)} = x_t^{(i)} - \gamma g_t^{(i)}$
5. Compute error compensated update  $v_t^{(i)} = \tilde{x}_t^{(i)} + \delta_t^{(i)}$
6. Compress the error compensated variable  $C[v_t^{(i)}]$  and update error  $\delta_t^{(i)} = v_t^{(i)} - C[v_t^{(i)}]$
7. Send  $C[v_t^{(i)}]$  and  $u_t^{(i)}$  to out-neighbours of  $i^{th}$  node (i.e. to  $j \in \mathcal{N}_i^{out}$ )
8. Receive  $C[v_t^{(j)}]$  and  $u_t^{(j)}$  from all the in-neighbours of  $i^{th}$  node ( $j \in \mathcal{N}_i^{in}$ )
9. Do the gossip update for local models and bias weights:  

$$x_{t+1}^{(i)} = \tilde{x}_t^{(i)} + \eta \sum_{j \in \mathcal{N}_i^{in}} (W_{ij} - I_{ij}) C[v_t^{(j)}]$$

$$u_{t+1}^{(i)} = u_t^{(i)} + \eta \sum_{j \in \mathcal{N}_i^{in}} (W_{ij} - I_{ij}) u_t^{(j)}$$
10. De-bias the updated model:  $z_{t+1}^{(i)} = \frac{x_{t+1}^{(i)}}{u_{t+1}^{(i)}}$
11. **end for**

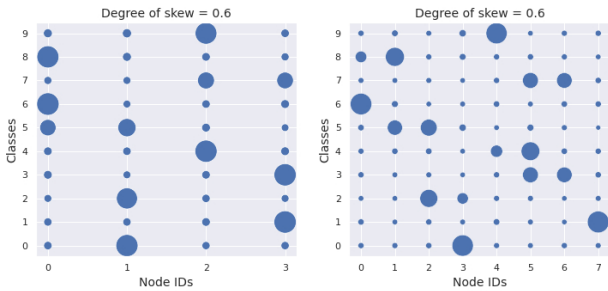


Figure 5. Data distribution of Imagenette dataset with a 0.6 degree of skew for a 4 node and a 8 node graph topologies.

## 8.2. Experimental Details

We have implemented our code in PyTorch and the GitHub link is provided in the abstract. We use stochastic gradient descent optimizer with nestrovo momentum and momentum hyper-parameter  $\beta = 0.9$ . For all the experiments, input samples were normalized before training and the usual data augmentation transformations such as random crop and random horizontal flip were applied to training data. We have used 2 different graph topologies for the decentralized setup namely directed ring and undirected

**Algorithm 5** Quant-SGP [18] (CHOCO-SGD with SGP)

**Input:** On each node  $i \in [n]$  - initialize model parameters  $x_0^{(i)}, z_0^{(i)} = x_0^{(i)}$ , initialize  $\hat{x}_0^{(j)} \forall j \in N(i)$  to 0s and bias weight  $u_0^{(i)}$  to 1, learning rate  $\gamma$ , averaging rate  $\eta$ , mixing matrix  $W$ , and compression operator  $C$ .

1. **for**  $t = 0, \dots, T - 1$ , at each node  $i$ , **do**  
Each node simultaneously implements:
2. Randomly sample mini-batch  $\xi_t^{(i)}$  from local distribution  $D_i$
3. Compute local gradient  $g_t^{(i)} = \nabla F_i(z_t^{(i)}, \xi_t^{(i)})$
4. Do the local update  $\tilde{x}_t^{(i)} = x_t^{(i)} - \gamma g_t^{(i)}$
5. Compute and compress the sending information:  
 $q_t^{(i)} = C[\tilde{x}_t^{(i)} - \hat{x}_t^{(i)}]$
7. Send  $q_t^{(i)}$  and  $u_t^{(i)}$  to out-neighbours of  $i^{th}$  node ( $\mathcal{N}_i^{out}$ )
7. **for** each neighbour  $j$  of  $i^{th}$  node ( $j \in \mathcal{N}_i^{in}$ ) **do**  
Receive  $q_t^{(j)}$  and  $u_t^{(j)}$   
 $\hat{x}_{t+1}^{(j)} = q_t^{(j)} + \hat{x}_t^{(j)}$
8. **end for**
9. Do the gossip update for local models and bias weights:  

$$x_{t+1}^{(i)} = \tilde{x}_t^{(i)} + \eta \sum_{j \in \mathcal{N}_i^{in}} (W_{ij} - I_{ij}) (\hat{x}_{t+1}^{(j)} - \hat{x}_{t+1}^{(i)})$$

$$u_{t+1}^{(i)} = u_t^{(i)} + \eta \sum_{j \in \mathcal{N}_i^{in}} (W_{ij} - I_{ij}) u_t^{(j)}$$
10. De-bias the updated model:  $z_{t+1}^{(i)} = \frac{x_{t+1}^{(i)}}{u_{t+1}^{(i)}}$
11. **end for**

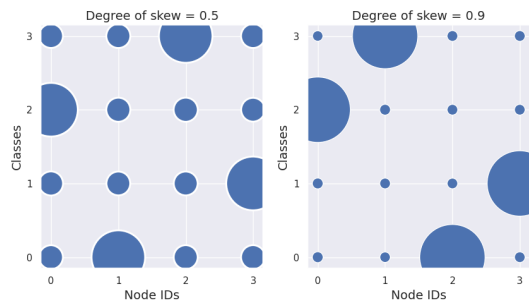


Figure 6. Data distribution of AG News dataset with a 0.5 and 0.9 degree of skew for 4 node ring topology.

torus as shown in Figure. 4. We evaluate the low precision training for various degree of skew (non-IID data partitions). A 0.0 degree of skew indicates the number of training samples across all the class are equally distributed for all the nodes. Increasing the degree of skew makes the distribution at each node to be skewed towards one or more classes. For CIFAR-10 dataset, we use three different non-zero degree of skews – 0.4, 0.8, 0.9 and the distribution of the classes across 8 node topology is shown in Figure. 2. For the non-IID case of Imagenette dataset, we evaluate on

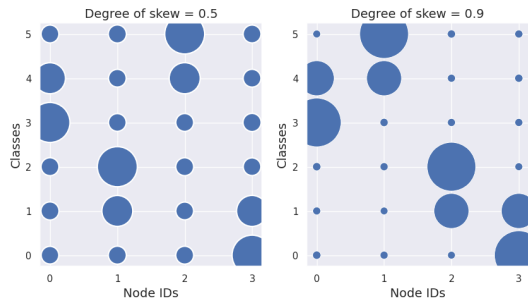


Figure 7. Data distribution of Sentlen dataset with a 0.5 and 0.9 degree of skew for 4 node ring topology.

0.6 degree of skew and the distribution of classes for a 4 node and a node graph topology is shown in Figure. 5. Similarly, Figure. 6, 7 show the distribution of classes with a skew of 0.5 and 0.9 for NLP datasets.